14.1 GBVTD-RETRIEVED NEAR-SURFACE AXISYMMETRIC VORTEX STRUCTURE IN A TORNADO AND IN TORNADO-LIKE VORTICES OBSERVED BY A W-BAND RADAR DURING VORTEX2

Robin L. Tanamachi[1,2,*]
Howard B. Bluestein[1]
Ming Xue[1,2]
Wen-Chau Lee[3]
Krzysztof A. Orzel[4]
Stephen J. Frasier[4]

[1]*School of Meteorology, University of Oklahoma, Norman, Oklahoma*
[2]*Center for Analysis and Prediction of Storms, University of Oklahoma, Norman, Oklahoma*
[3]*National Center for Atmospheric Research, Boulder, Colorado*
[4]*Microwave Remote Sensing Laboratory, University of Massachusetts, Amherst, Massachusetts*

1. INTRODUCTION

In this study, we explore the weak end of the tornado spectrum (≤EF1) by analyzing two similar vortices that occurred one day apart during VORTEX2 (Wurman et al. 2012). The first, which occurred in a supercell near Tribune, Kansas on 25 May 2010 (hereafter "the Tribune storm"), was an unequivocal tornado. The second vortex was observed in a supercell near Prospect Valley, Colorado on 26 May 2010 (hereafter "the Prospect Valley storm") and was more resistant to the conventional definition of a tornado (e.g., Glickman 2000). High-resolution Doppler velocity observations were collected below 200 m AGL in these two vortices by the University of Massachusetts mobile, W-band, Doppler radar ("UMass W-band" hereafter; Tsai et al. 2008).

Vortex-relative radial and azimuthal winds in tornadoes observed by mobile Doppler radar can potentially be retrieved using the Ground-Based Velocity Track Display (GBVTD; Lee et al. 1999) technique (Bluestein et al. 2003; Lee and Wurman 2005; Bluestein et al. 2007; Tanamachi et al. 2007; Kosiba et al. 2008; Kosiba and Wurman 2010; Metzger et al. 2011; Chan et al. 2012; Wakimoto et al. 2012). In this study, we apply the GBVTD technique to retrieve winds from UMass W-band observations of a tornado in the Tribune storm and in a tornado-like vortex (TLV) in the Prospect Valley storm. A TLV is herein defined as a radar data feature having many of the same characteristics as a tornado, including a persistent reflectivity spiral, weak-echo hole (WEH), and vortex signature (VS), but which is *not* accompanied by a visible condensation funnel. Bluestein et al. (2001) documented similar weak vortices observed by the UMass W-band radar in the hook echoes of two different supercells in 2000; these vortices appear to conform to the definition of a TLV given above.

Questions guiding this study are as follows: Are there significant differences in the near-surface structures of the vortices observed by UMass W-band on 25 May and 26 May? How are the GBVTD-retrieved winds related to the visual appearance of the vortex? What are the implications for the conventional definition of a tornado?

2. OBSERVATIONS BY THE UMASS W-BAND RADAR

A full description of the UMass W-band radar can be found in Tsai et al. (2008). This radar has an exceptionally narrow beamwidth (0.18°), a range resolution of 30 m, and an effective maximum unambiguous velocity of 38 m s^{-1}. However, it is limited to a maximum range of 12.3 km principally by the rapid attenuation of 3.2 mm wavelength signal in precipitation. During VORTEX2, the mission of the UMass W-band radar, which had the highest spatial resolution of all the radars in the "armada," was to collect close-range, near-surface Doppler radar observations beneath the hook echoes of supercells.

The Tribune storm (25 May 2010)

On the afternoon of 25 May 2010, the Tribune storm produced several tornadoes as it tracked from southeast Colorado into

* *Corresponding author's current affiliation*: Robin L. Tanamachi; National Severe Storms Laboratory; 120 David L. Boren Blvd.; Norman, OK 73072; e-mail: rtanamachi@ou.edu

western Kansas (Monteverdi et al. 2010), including at least four observed by one of the authors (H. Bluestein). The VORTEX2 team targeted and intercepted this storm near Tribune, Kansas at 2300 UTC, collecting data in two tornadoes that it produced. UMass W-band deployed 23 km west of Tribune at 2310 UTC, scanning the hook region of the Tribune storm (which was about 8 km to north of UMass W-band) at about 100 m AGL. At 2314 UTC, a funnel cloud (funnel 1; not shown) extended downward to contact the ground briefly, lasting three minutes before dissipating. It was followed by another, wider, cloud-to-ground condensation funnel (funnel 2) at 2320 UTC that also lasted three minutes (Fig. 1a). A reflectivity spiral, WEH likely generated by centrifuging (Dowell et al. 2005) (Fig. 2a, c, e) and VS (Fig. 2b, d, f) are all present in the UMass W-band data continuously from 2314 UTC to 2323 UTC. We therefore consider the two condensation funnels to be separate visual incarnations of the same tornado.

The Prospect Valley storm (26 May 2010)

VORTEX2 teams converged on this storm near Prospect Valley, Colorado (northeast of Denver) around 2150 UTC. The teams observed a shallow, bowl-shaped lowering of the cloud base that persisted for more than 30 minutes (Fig. 1b), but no tornado or funnel cloud was observed or reported. Many groups collected an hour or more of continuous observations as the storm moved slowly to the northeast at 5 to 6 m s^{-1}. Operations ended at 0041 UTC on 27 May.

The UMass W-band radar deployed 18 km south of Wiggins, Colorado, and scanned the Prospect Valley storm's hook echo from a range of 4 to 8 km at an elevation angle of 1.9°. During the period of greatest interest (2217-2247 UTC), the beam was 150-250 m AGL. The hook echo exhibited complex reflectivity structure, including a fine line – possibly the leading edge of the rear-flank gust front – extending eastward from the tip of the hook (Fig. 3). Some of the TLVs occurred at the intersection of the fine line and the tip of the hook echo, possibly indicating that their origins lay in shear instability along the fine line. At least seven TLVs, all cyclonic and lasting at least 1 min, were identified in the UMass W-band data (5 and 6 are shown in Fig. 3). The TLVs consistently developed either to the southeast or south of an associated mesocyclone at 1 km AGL detected by MWR-05XP and other radars (not shown).

The strongest and longest-lived of these TLVs (5) appeared at the tip of the hook at 2234 UTC, 4.5 km from UMass W-band (Fig. 4), near the intersection with the fine line (Fig. 3c, d). In the W-band radar data set, TLV 5 bears a strong resemblance to the radar depiction of the Tribune tornado, with many similar features including a persistent (8-min) WEH (Fig. 4a, c, e) and VS (Fig. 4b, d, f). At 2242 UTC, TLV 5 dissipated when the WEH filled in with precipitation and the VS weakened. In our GBVTD analyses, we focus principally on TLV 5 because of its similarity in size, structure, and duration (8 min) to the Tribune tornado observed the preceding day.

3. METHODOLOGY

Because both vortices were relatively weak, manual dealiasing of the velocity data was not needed. The UMass W-band data were objectively analyzed to a Cartesian grid centered on the vortex using a two-pass Barnes (1964) scheme. Only one vertical grid level was used because the UMass W-band data were collected at only one elevation angle. The horizontal grid spacing for the 25 May (26 May) case was 12 m (10 m) (Koch et al. 1983; Trapp and Doswell 2000). During objective analysis, a time-to-space conversion, based on the estimated motion of the WEH, was applied to the data in order to minimize translational distortion of the vortex (Tanamachi et al. 2007).

The centers of the vortices were located in the objective analyzed Doppler velocity data using the simplex center-seeking algorithm of Nelder and Mead (1965), as adapted by Lee and Marks (2000). Finally, from the objectively analyzed Doppler velocity data and the vortex center at each analysis time, the GBVTD algorithm (Lee et al. 1999) calculated vortex-centered wavenumber-0 (axisymmetric), -1, -2, and -3 azimuthal velocity components (V_{T0}, V_{T1}, V_{T2}, and V_{T3}, respectively), as well as the axisymmetric radial velocity component (V_{R0}). Hereafter, we focus on the V_{T0}, which would have been less affected by noise and centrifuging than the V_{R0} or higher-wavenumber V_Ts.

The Tribune data suffered from an elevated noise floor, which the authors attribute to a temporary malfunction of the UMass W-band low-noise amplifier. It is accepted that there will be some errors in the GBVTD analyses of the 25 May data resulting from the elevated noise floor. However, the analyzed axisymmetric vortex structures appear similar to those of previously analyzed tornadoes. We therefore consider the structures credible, and proceed to describe them in the next section.

4. RESULTS

The Tribune storm (25 May 2010)

In general, the V_{T0} winds increased (decreased) at all radii in concert with the appearance (disappearance) of the tornado condensation funnel (Fig. 5). Circulation and vorticity inside a 200 m radius (not shown) also exhibited this trend. Assuming the thermodynamic properties of ingested air remain relatively constant, a condensation funnel forms in response to increasing wind speeds and a dynamic pressure drop inside the vortex, where water vapor condenses into cloud droplets. The appearance of a condensation funnel, therefore, serves as a visual indicator of vortex intensification. The consistent association between changes in analyzed wind speeds and the appearance or disappearance of the condensation funnel lends confidence to the analyzed trends in V_{T0}.

We compared these results to analyzed V_{T0} in the 5 June 1999 Bassett, Nebraska tornado (Bluestein et al. 2003) and the 15 May 1999 Stockton, Kansas tornado (Tanamachi et al. 2007). In terms of peak V_{T0}, the Tribune tornado was both wider (230 m radius) and weaker (19 m s^{-1}; F0) than either the Bassett (140 m; 30 m s^{-1}; F0) or Stockton (80 m; 45 m s^{-1}; F1) tornadoes. The intermittent appearance of the condensation funnel leads us to believe that the available moisture was barely adequate for the formation of the condensation funnel.

Prior to tornadogenesis (2314 UTC), we have low confidence in the RMW (taken as the radius of peak V_{T0}; Fig. 6a) because the tip of the hook contained little precipitation (not shown). The RMW fluctuated around 300 m when funnel 1 was visible (2314-2317 UTC). The RMW decreased to about 200 m as funnel 2 formed (2320-2323 UTC), then increased again to more than 300 m as funnel 2 dissipated. The trend of decay via increasing RMW and decreasing V_{T0} is consistent with analyses of the Bassett tornado by Bluestein (2003), but contrasts with results from Tanamachi et al. (2007), who found that RMW decreased in the decaying Stockton tornado. The Tribune tornado appears to have been more like the Bassett tornado than the Stockton tornado in most regards.

The Prospect Valley storm (26 May 2010)

We analyzed the UMass W-band data collected in TLV 5 in exactly the same manner as we did previous UMass W-band tornado data sets. GBVTD analysis was possible once the developing TLV 5 (initially scatterer-free) was completely encircled by scatterers at genesis (2234 UTC), leaving a WEH in the middle (Fig. 4a).

Lacking a condensation funnel to use as an indicator of vortex intensification, we instead used the presence of a WEH. Over its 8 min life cycle, TLV 5 intensified and then decayed similarly to previously analyzed tornadoes (Fig. 7). V_{T0} generally increased (decreased) at all radii when TLV 5 intensified (weakened). Maximum V_{T0} analyzed in TLV 5 was 13 m s^{-1} (Fig. 6b), weaker than that analyzed in the Tribune, Bassett, or Stockton tornadoes.

The RMW shrank to less than 100 m as TLV 5 intensified (2234 to 2238 UTC), then increased beyond 200 m after the WEH closed at 2240 UTC (Fig. 6b). This inverse relationship of V_{T0} and RMW is consistent with that found in previously-analyzed tornadoes, including the Tribune tornado.

5. CONCLUSIONS

High-resolution (~10 m) GBVTD analyses were conducted on two W-band radar data sets collected in the hook echoes of tornadic supercells during VORTEX2. The two data sets, collected one day apart and at 150 m AGL or lower, show the full life cycle of an EF-0 tornado in western Kansas and a TLV, which did not have an associated condensation funnel, in northeast Colorado.

It was found that the Tribune tornado and Prospect Valley TLV 5 both had similar life spans (as measured by the appearance of WEHs, ~8 min), similar intensification and weakening phases (as seen in the evolution of the V_{T0}, RMW, circulation / angular momentum, and vorticity), and similar axisymmetric vortex structure at peak intensity. A VS and WEH are clearly visible in the UMass W-band data collected in TLV 5 on 26 May 2010 and bear a strong resemblance to those seen the Tribune tornado seen the previous day.

The principal differences between these two vortices lay in the speed of the azimuthal winds (which were smaller for the TLV), the RMW (which was wider in the Tribune tornado), and the absence of a condensation funnel in TLV 5, which we attribute to insufficient moisture below cloud base.

TLV 5 appears, for all intents and purposes, to have been a weak, invisible tornado. It is well known that a tornado with no visible condensation funnel can still inflict surface damage (although none was documented in this case). TLV 5 occurred in conjunction with other features frequently accompanying mesocyclonic tornadoes (e.g., a clear slot, DRCs). Therefore, the authors feel it is unlikely that TLV 5 was a non-mesocyclonic vortex or a “gustnado.” On the other hand, more than 100 VORTEX2 personnel, most of whom had at least some tornado field research experience, were present during the data collection. It is remarkable that none reported a tornado or even a funnel cloud, only a “suspicious lowering” of the cloud base (Fig. 1b).

While the peak analyzed V_{T0} in the Prospect Valley TLV 5 was only 13 m s^{-1} (Fig. 6b), peak analyzed V_{T0} in the Tribune, Bassett, and Stockton tornadoes approached or even dipped below this value at some point during their life cycles. Similar velocities were measured by UMass W-band at inner radii in both the Tribune tornado and TLV 5. Therefore, the distinction between a tornado and a TLV may be merely a matter of moisture. While the tornado and TLV analyzed here could be considered minimal tornadoes, the results of the GBVTD analyses suggest that they share many features in common with stronger tornadoes. We suspect that many such TLVs occur beneath High Plains supercells, but go unreported for the simple lack of a visual indicator such as a condensation funnel or debris cloud. It is only through the use of high-resolution radars such as the UMass W-band and Texas Tech University Ka-band mobile radars (Hirth et al. 2012) that such vortices can be detected and documented.

6. ACKNOWLEDGMENTS

This study was primarily supported by National Science Foundation (NSF) grant ATM-0802888. The UMass W-band radar data collection during VORTEX2 was supported by NSF grants ATM-0934307, ATM-0641201, and AGS-0937768. Observation Processing and Wind Synthesis (OPAWS; http://code.google.com/p/opaws/) software created by Drs. David Dowell and Louis Wicker was used for the objective analyses. Drs. Phillip Stauffer and Michael Bell updated the GBVTD code. Sounding and mobile mesonet data from VORTEX2 were provided by the National Center for Atmospheric Research Earth Observing Laboratory (NCAR / EOL) under sponsorship of the NSF.

7. REFERENCES

Barnes, S. L., 1964: A technique for maximizing details in numerical weather map analysis. *J. Appl. Meteor.*, **3,** 396-409.

Bluestein, H. B., C. C. Weiss, and A. L. Pazmany, 2001: Observations in supercells with a mobile, 3-mm wavelength Doppler radar. *30th International Conf. on Radar Meteorology*, Munich, Germany, American Meteorological Society, 292-294.

Bluestein, H. B., W.-C. Lee, M. Bell, C. C. Weiss, and A. L. Pazmany, 2003: Mobile Doppler radar observations of a tornado in a supercell near Bassett, Nebraska, on 5 June 1999. Part II: Tornado-vortex structure. *Mon. Wea. Rev.*, **131,** 2968-2984.

Bluestein, H. B., C. C. Weiss, M. M. French, E. M. Holthaus, R. L. Tanamachi, S. Frasier, and A. L. Pazmany, 2007: The structure of tornadoes near Attica, Kansas, on 12 May 2004: High-resolution, mobile, Doppler radar observations. *Mon. Wea. Rev.*, **135,** 475-506.

Chan, P. W., J. Wurman, C. M. Shun, P. Robinson, and K. Kosiba, 2012: Application of a method for the automatic detection and Ground-Based Velocity Track Display (GBVTD) analysis of a tornado crossing the Hong Kong International Airport. *Atmos. Res.*, **106,** 18-29.

Dowell, D. C., C. R. Alexander, J. M. Wurman, and L. J. Wicker, 2005: Centrifuging of hydrometeors and debris in tornadoes: Radar-reflectivity patterns and wind-measurement errors. *Mon. Wea. Rev.*, **133,** 1501-1524.

Glickman, T. S., 2000: *Glossary of Meteorology.* 2nd ed. American Meteorological Society, 855 pp.

Hirth, B. D., J. L. Schroeder, W. S. Gunter, and J. G. Guynes, 2012: Measuring a utility scale turbine wake using the TTUKa mobile research radars. *J. Atmos. Oceanic Technol.*, **29,** 765-771.

Koch, S. E., M. desJardins, and P. J. Kocin, 1983: An interactive Barnes objective map analysis scheme for use with satellite and conventional data. *J. Climate Appl. Meteor.*, **22,** 1487-1503.

Kosiba, K., and J. Wurman, 2010: The three-dimensional axisymmetric wind field structure of the Spencer, South Dakota, 1998 tornado. *J. Atmos. Sci.*, **67,** 3074-3083.

Kosiba, K. A., R. J. Trapp, and J. Wurman, 2008: An analysis of the axisymmetric three-dimensional low level wind field in a tornado using mobile radar observations. *Geophys. Res. Lett.*, **35,** L05805.

Lee, W.-C., and F. D. Marks, 2000: Tropical cyclone kinematic structure retrieved from single-Doppler radar observations. Part II: The GBVTD-simplex center finding algorithm. *Mon. Wea. Rev.*, **128,** 1925-1936.

Lee, W.-C., and J. Wurman, 2005: Diagnosed three-dimensional axisymmetric structure of the Mulhall tornado on 3 May 1999. *J. Atmos. Sci.*, **62,** 2373-2393.

Lee, W.-C., B. J.-D. Jou, P.-L. Chang, and S.-M. Deng, 1999: Tropical cyclone kinematic structure retrieved from single-Doppler radar observations. Part I: Interpretation of Doppler velocity patterns and the GBVTD technique. *Mon. Wea. Rev.*, **127,** 2419-2439.

Metzger, R. S., C. C. Weiss, and A. E. Reinhart, 2011: An examination of the structure of three tornadoes using high-frequency Ka-band mobile doppler radar. *35th Conference on Radar Meteorology*, Pittsburgh, Pennsylvania, American Meteorological Society, 7B.4.

Monteverdi, J. P., M. M. Umscheid, and E. M. Bookbinder, 2010: Two tornadic thunderstorms in ostensibly weak deep layer shear environments in southeastern Colorado: cyclic supercells of May 25 (Kiowa County) and May 31 (Baca County) 2010. *25th Conf. on Severe Local Storms*, American Meteorological Society, P10.14.

Nelder, J. A., and R. Mead, 1965: A simplex method for function minimization. *Comput. J.*, **7,** 308-313.

Tanamachi, R. L., H. B. Bluestein, W.-C. Lee, M. Bell, and A. Pazmany, 2007: Ground-Based Velocity Track Display (GBVTD) analysis of W-Band Doppler radar data in a tornado near Stockton, Kansas, on 15 May 1999. *Mon. Wea. Rev.*, **135,** 783-800.

Trapp, R. J., and C. A. Doswell, 2000: Radar data objective analysis. *J. Atmos. Oceanic Technol.*, **17,** 105-120.

Tsai, P., S. Frasier, R. L. Tanamachi, and H. B. Bluestein, 2008: The UMass mobile W-Band Doppler radar: System overview and sample observations. *24th Conf. on Severe Local Storms*, Savannah, Georgia, American Meteorological Society, P13.15.

Wakimoto, R. M., P. Stauffer, W.-C. Lee, N. T. Atkins, and J. Wurman, 2012: Finescale structure of the LaGrange, Wyoming tornado during VORTEX2: GBVTD and photogrammetric analyses. *Mon. Wea. Rev.*, **140,** 3397–3418.

Wurman, J., D. Dowell, Y. Richardson, P. Markowski, E. Rasmussen, D. Burgess, L. Wicker, and H. B. Bluestein, 2012: The Second Verification of the Origins of Rotation in Tornadoes Experiment: VORTEX2. *Bull. Amer. Meteor. Soc.*, **93,** 1147-1170.

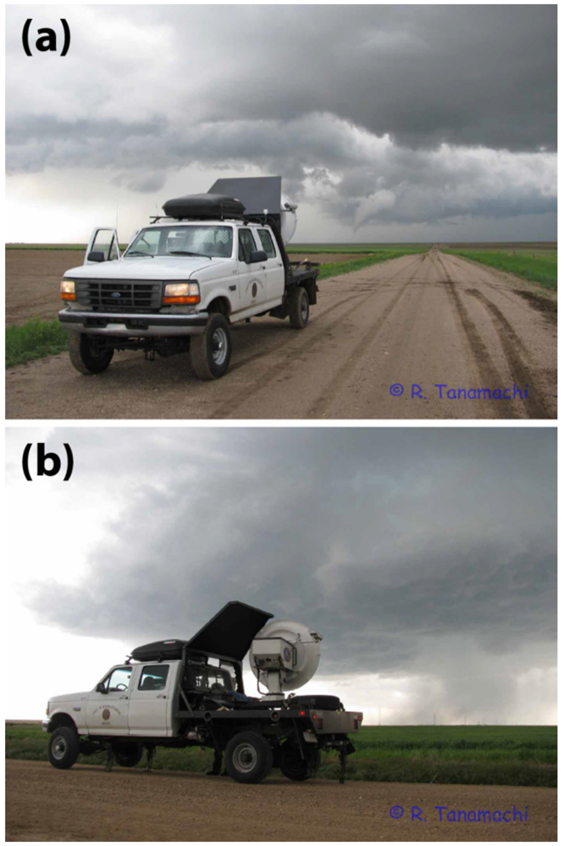

Fig. 1. The UMass W-band radar collects reflectivity and Doppler velocity data in (a) an EF-0 tornado in the Tribune, Kansas supercell at 2316 UTC on 25 May 2010, and (b) the hook echo region of the Prospect Valley, Colorado supercell at 2215 UTC on 26 May 2010. The view is toward (a) the north, and (b) the west.

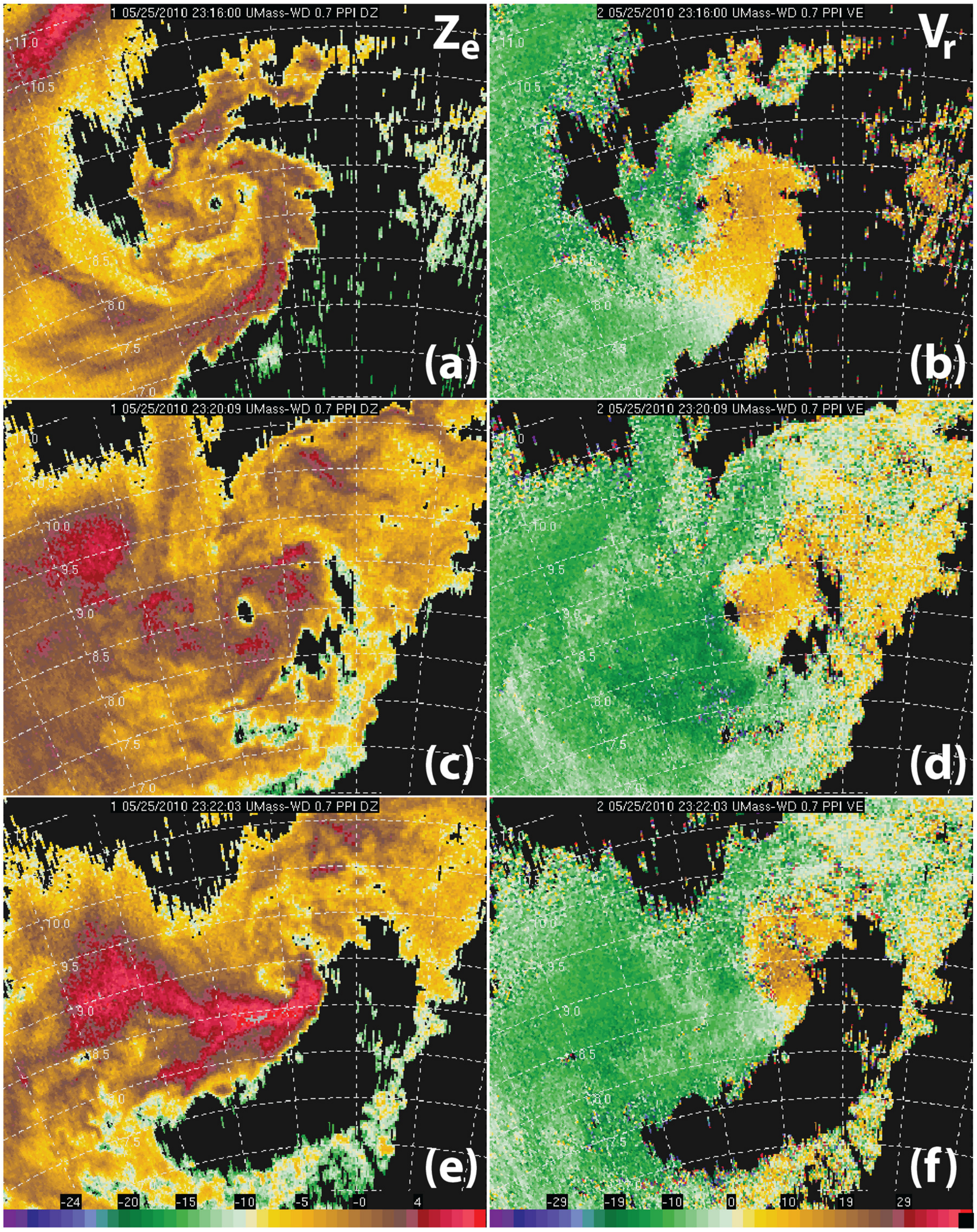

Fig. 2. (left column) Equivalent reflectivity (in dBZ_e) and (right column) Doppler velocity observed by the UMass W-band radar at an elevation angle of 0.7° in the 25 May 2010 Tribune, Kansas tornado at (a, b) 2316 UTC, (c, d) 2320 UTC, and (e, f) 2322 UTC. The images shown represent (a, b) mature funnel 1, (c, d) formation of funnel 2, (e, f) dissipation of funnel 2. Range rings (azimuth spokes) are 0.5 km (5°) apart. For clarity, data associated with signal-to-noise ratio (SNR) less than -10 dB are masked.

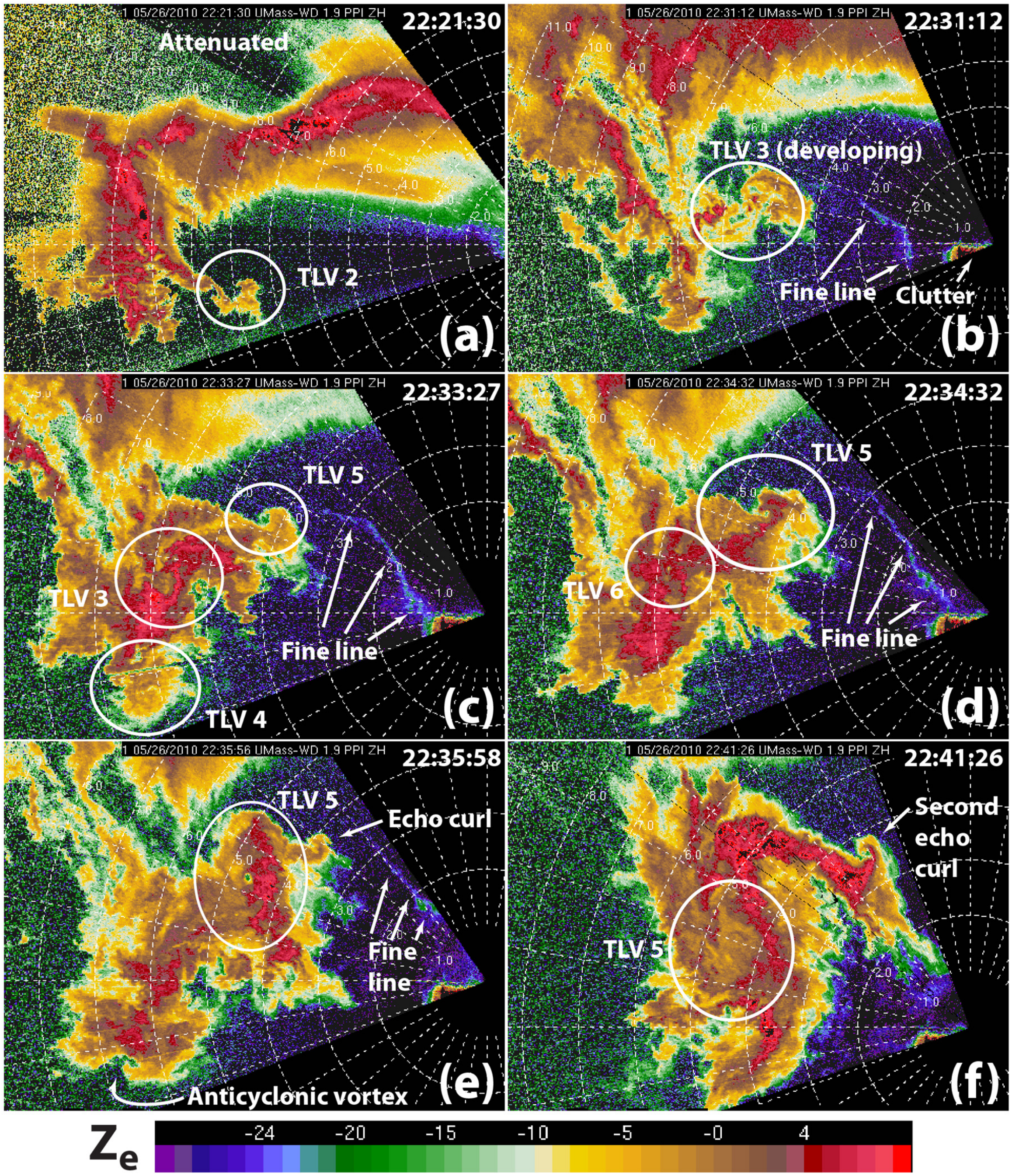

Fig. 3. UMass W-band equivalent reflectivity (in dBZ$_e$) at an elevation angle of 1.9° in the 26 May 2010 Prospect Valley storm, showing the evolution of the hook echo and gust front structures. A few echo curls not associated with significant vorticity are also annotated. Range rings (azimuth spokes) are 1.0 km (10°) apart.

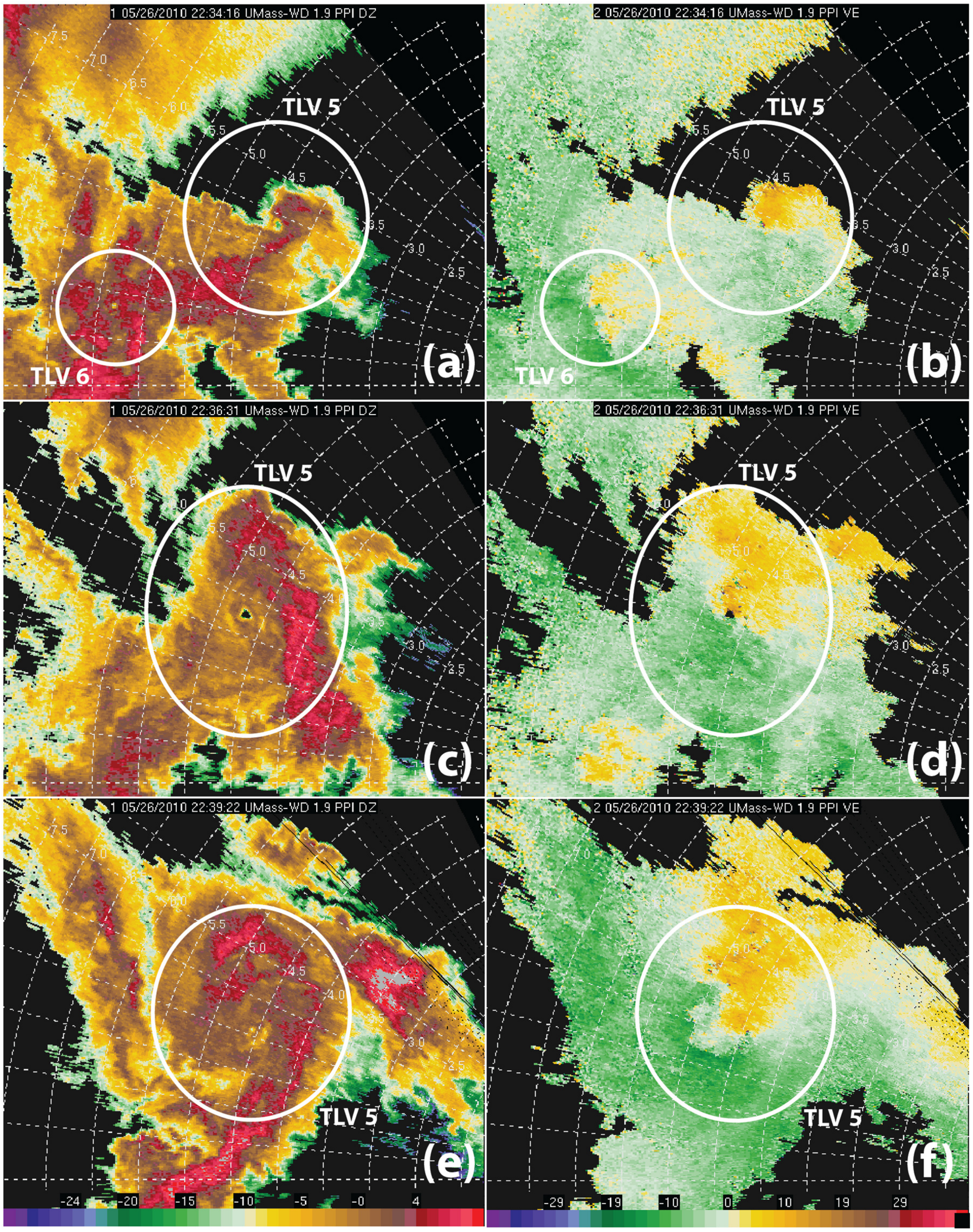

Fig. 4. As in Fig. 2, but focused on the 26 May 2010 Prospect Valley, Colorado TLV 5 (circled) at an elevation angle of 1.9° at (a, b) 2234 UTC, (c, d) 2237 UTC, and (e, f) 2239 UTC. For clarity, data associated with signal-to-noise ratio (SNR) less than -6 dB are masked. Panels (a), (c), and (d) detail some of the data shown in Fig. 3.

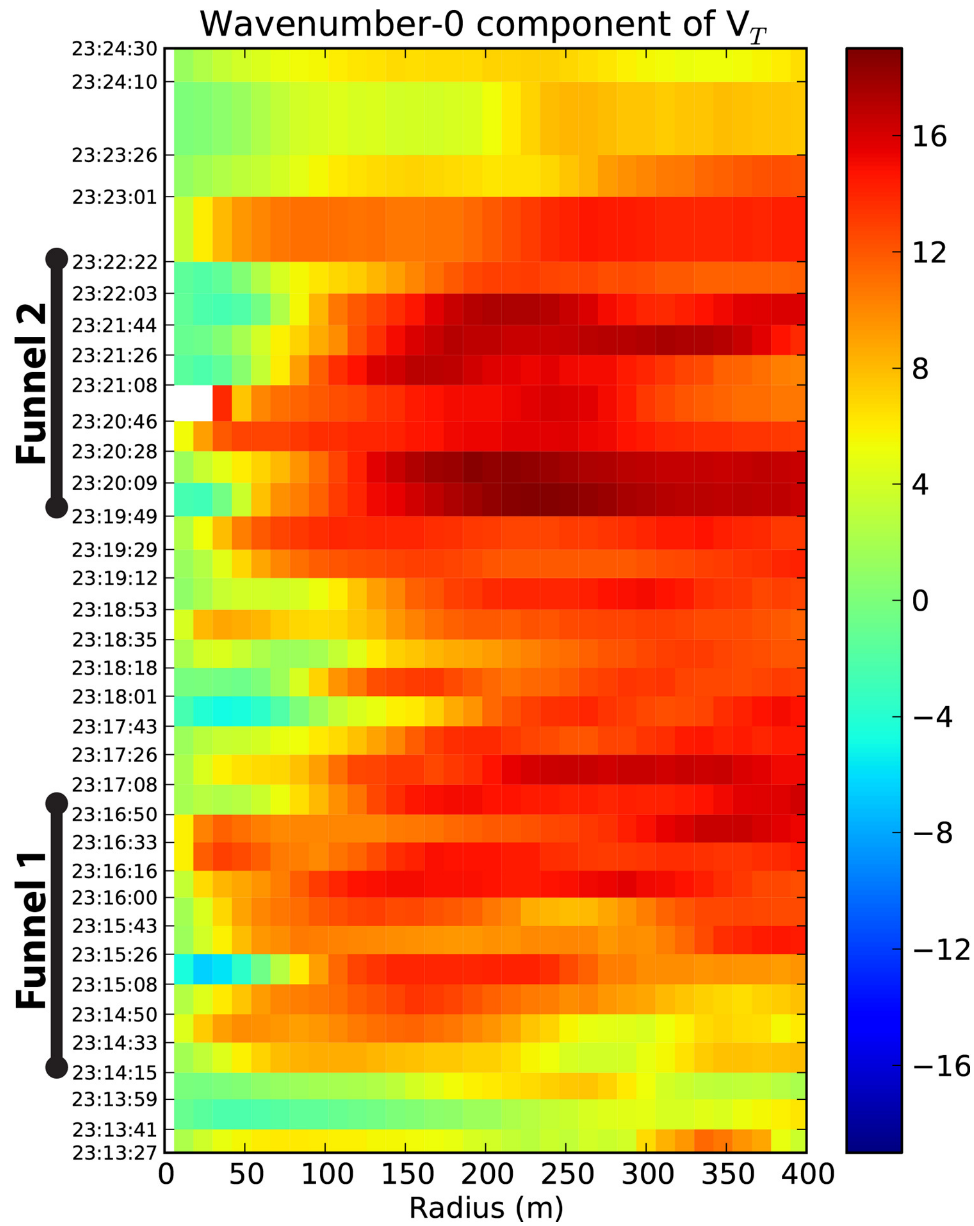

Fig. 5. Hovmöller diagram of GBVTD-analyzed V_{T0} (in m s^{-1}) in the Tribune tornado as a function of radius. Visible condensation funnels are denoted on the vertical axis.

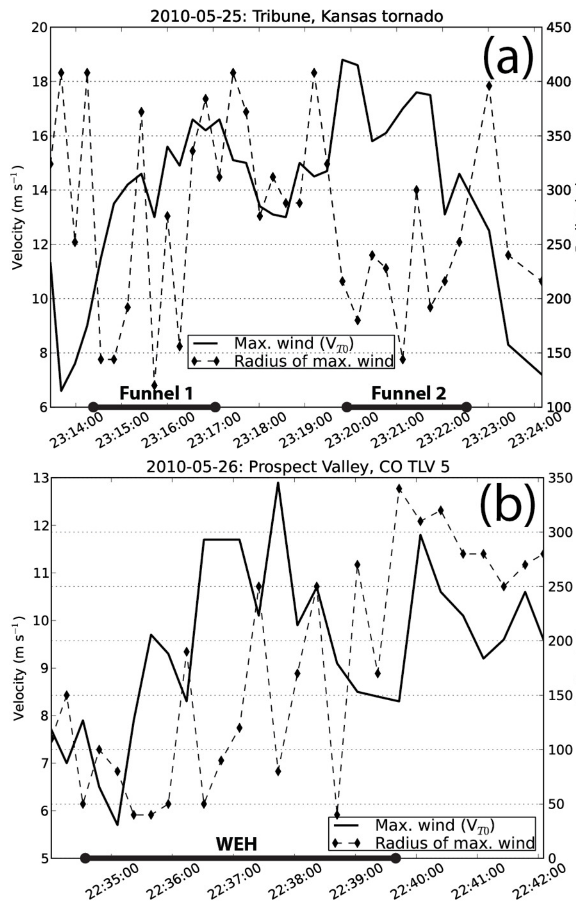

Fig. 6. (a) Maximum V_{T0} (solid line, in m s^{-1}) and radius of maximum V_{T0} (dashed line, in m) analyzed in the Tribune tornado. The appearances of condensation funnels are annotated on the horizontal axis. (b) As in panel (a), but for Prospect Valley TLV 5. The presence of the WEH is annotated on the horizontal axis.

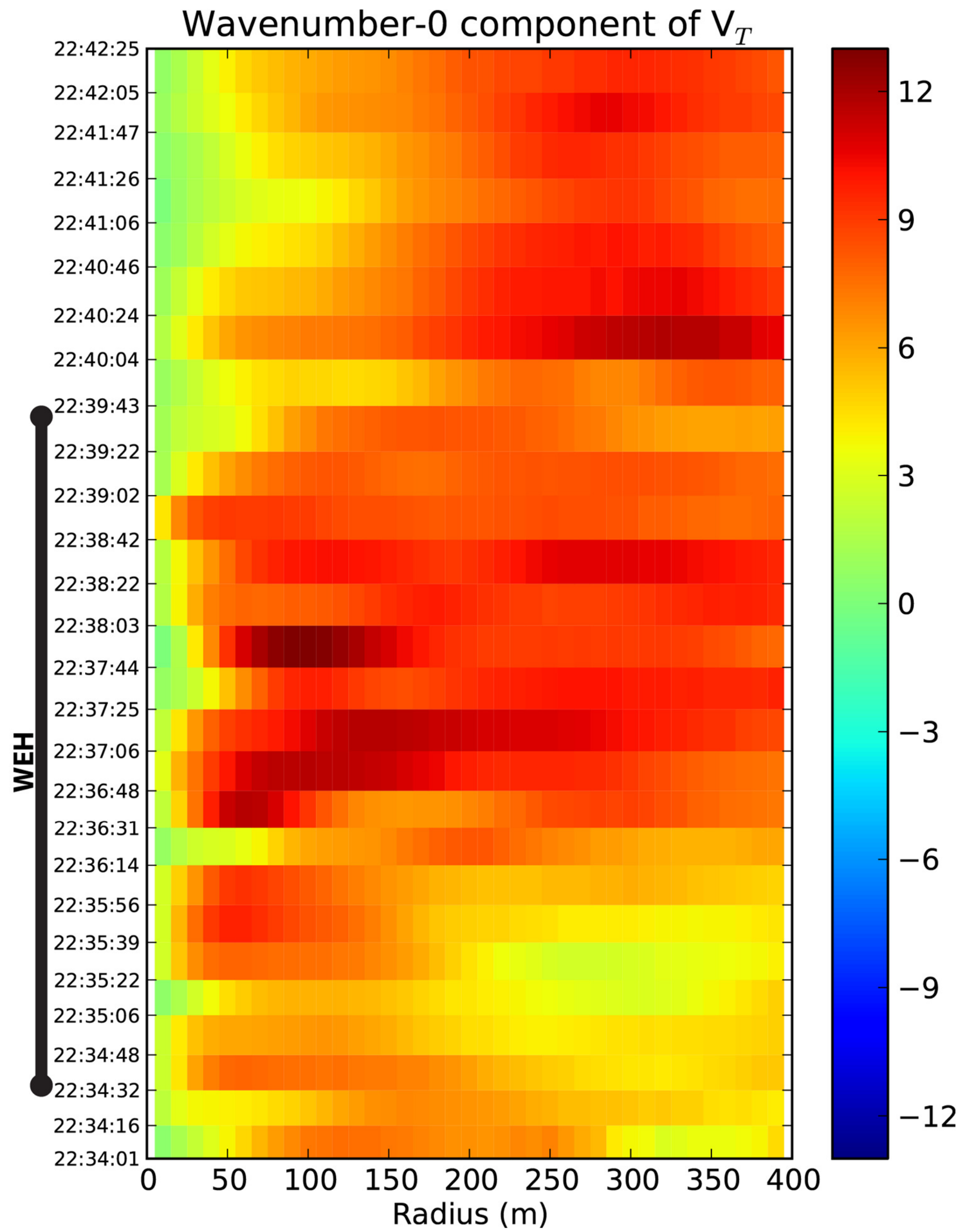

Fig. 7. Same as Fig. 5, but for Prospect Valley TLV 5. The presence of the WEH is annotated on the vertical axis.